Dual-Wavelength Pumping of Photonic Crystal Fibers

[1]Akhilesh Kumar Chauhan, [2]Shailesh Kumar Singh
[1]M.Sc. Student Monad University, Hapur
[2]Head and Professor Monad University Hapur

Abstract : Dual-wavelength pumping of PCFs has shown to enable broadband optimistic light sources with high spectral concentration in the visible. Investigates with femto-second pulses, in arrangement with numerical simulations, show that the major mechanism is XPM of the observable pulse executed by vital solitons. The group velocity discrepancy between XPM-shifted constituents and red-shifting solitons basis sequential walk-off and thereby a stable XPM-shift in spite of full walk-through of the soliton. Dual-pump experiments with picosecond and nanosecond pulses gave similar results as the ones obtained with femtosecond pumping. It is well known that modulation doubts cause longer pump pulses to break up into shorter pulses which evolve into soliton so the only difference between the three pumping systems is actually the number of interacting solitons. The use of dual-wavelength pumping of PCFs has allowed original picosecond and nanosecond white-light sources and has previously led to the commercially available Super K white light source. Since the effect of dual-wavelength pumping is governed by the choice of pump wavelengths and the group delays in the used.

IndexTerms - red-shifting, K white light source, XPM-shifted

I. INTRODUCTION

Commonly SCG in micro structured fibers has been acquired by pumping the fiber in the uncharacteristic dispersion regime where fission of solitons delivers a wide spectrum over SPM, Raman-scattering and FWM. The fission of a higher order soliton into its constituent fundamental solitons also gives rise to growth of dispersive waves which are regularly establish deep in the visible. However, it was recently described that extraordinary wide and flat spectra could be attained in the visible by simultaneously pumping a PCF in the normal and anomalous regime with picosecond pulses. By co-propagating the second harmonic (SH) at 532 nm and the fundamental at 1064 nm it was found that the discrete Raman lines in the visible were smoothened out, subsequent in a flat spectrum adjusted at 532 nm. This was assumed to source from an capture of stimulated Raman scattering (SRS) due to a four wave collaborating (FWM) progression which, in case of phase matching, has higher gain. The demonstration of a broadband visible light source with a simple setup, spurred interest in dual-wavelength pumping of photonic crystal fibers and it was later suggested that co-propagating two femto-second pulses could lead to major spectral broadening of the SH pulse due to cross phase modulation (XPM) imposed by necessary solitons. Simulations showed that a co-propagating SH pulse at 450 nm could be broadened with more than 100 nm in this way. In this chapter, it is demonstrated experimentally that femtosecond dual pumping indeed leads to a spectral broadening of the co-propagating SH pulse due to cross phase modulation.

II. EXPERIMENTAL SETUP

The experimental setup is shown in figure 1. An Yb: KGW oscillator is delivering 1028 nm, transform-limited 380 femto-second pulses at a replication rate of 9.8 MHz and a pulse energy up to 250 n J. The pulses are frequency doubled up in a 17 mm long LBO (Lithium Triborate) crystal with an efficacy of up to 60%. The fundamental and second harmonic beams are then separated with a dichroic mirror reflecting 1028 nm and transmitting 514 nm. Each beam is re-collimated and sent through appropriate telescopes in order to ensure proper mode matching at the position of the fiber tip. The IR beam is sent through a delay stage before it is recombined with the SH and coupled into 35 cm of the PCF. Using a regular aspheric lens with a focal length of 4.5 mm it is possible to get approximately 30 % of both colors through the fiber simultaneously. After the fiber, an achromatic microscope objective collimate the super continuum. The fiber is passing ringent and half-wave plates are used to ensure that both beams are coupled into the main axis of the fiber. Temporal overlap is conveniently found by observing the spectrum diffracted off a grating onto a white when the pulses intersection in the fiber, intense visible components appear in the spectrum. Depending on the position of the stage, red or blue frequency components can be emphasized as illustrated in figure 2.
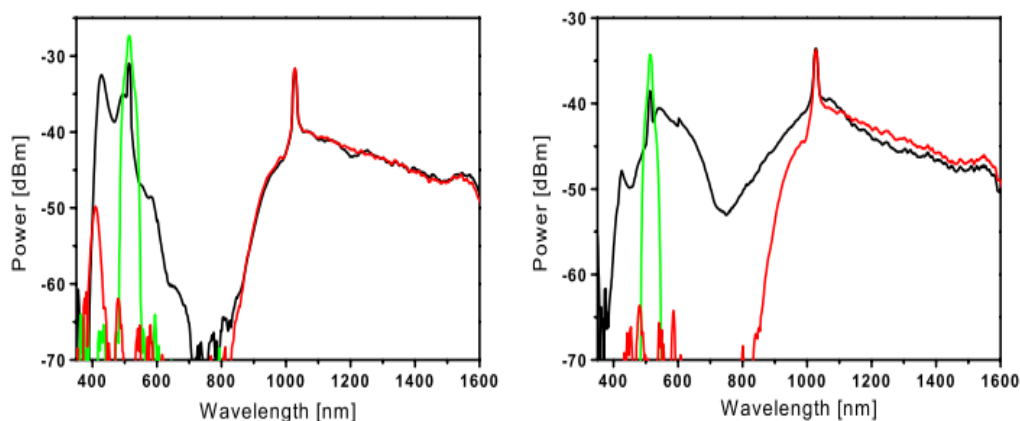

Figure 2: Black curve shows the enhancement of the blue (left) and red side (right) of the XPM shifted SH signal. Green and red curves represent the isolated SH and fundamental signals respectively. In both figures the IR pump power is 20 mW and the SH power is 12 mW.

RESULTS

Figure 2 shows the dramatic effect of launching two pulses into the PCF. Red curves show the spectrum of the fundamental IR pulse in absence of the SH pulse, green curves show the 514 nm pulse alone and black curves show the result of the interaction of two pulses. In the left figure, the temporal overlap is adjusted to optimize the blue part of the spectrum while the red part is optimized in the right figure. In both figures, the fundamental pulse alone causes a broad spectrum in the infrared due to SRS and also weak NSR around 420 nm.
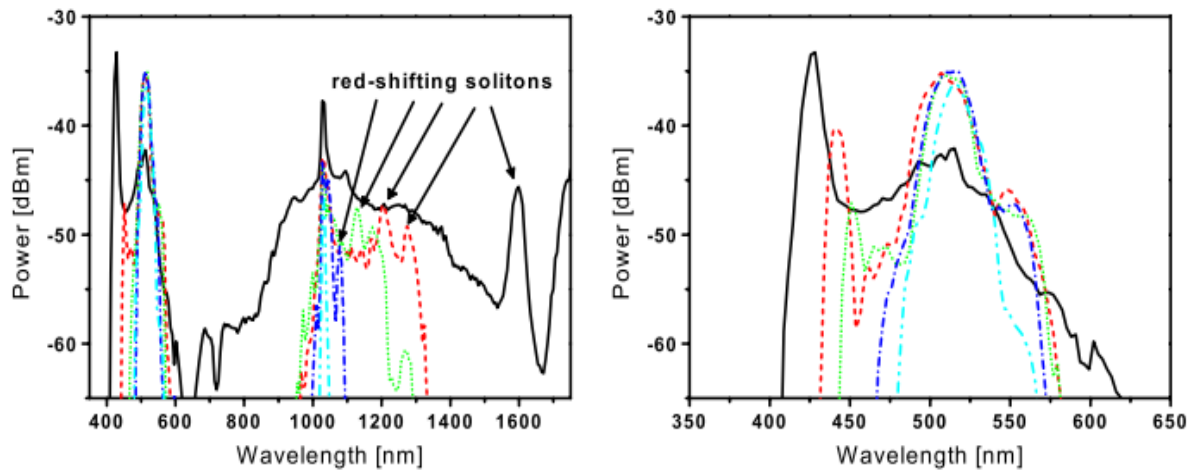

Figure.3: Left: Spectral evolution as function of increasing IR power. Maximum IR power is 18 mW and the green power is constant at 6 mW. Right: Same evolution in the spectral range close to the SH pump. Cascaded XPM leads to a large blue-shift of the green pulse.

When the SH pulse is launched into the fiber, the visible part of the spectrum is shifted almost 100 nm towards the blue (left figure). In the right figure, the 514 nm pulse is red shifted and the visible part of the spectrum almost merges with the NIR part. Figure 3 shows the spectral evolution as function of IR input power in more detail. The visible pump power is kept constant at 6 mW (0.67 n J) and the IR power is gradually increased but kept below the threshold for emission of NSR in order to highlight the effect of the dual pumping. The left figure shows how increased IR power leads to red-shifting of the solitons and finally emergence of several fundamental solitons. In figure 3 (right) a significant blue-shift is observed with increasing pump power. Integration of the spectra shows energy conservation in the spectral range 350 nm – 650 nm, so there is not energy transfer between pulses. This indicates that the underlying mechanism is XPM.
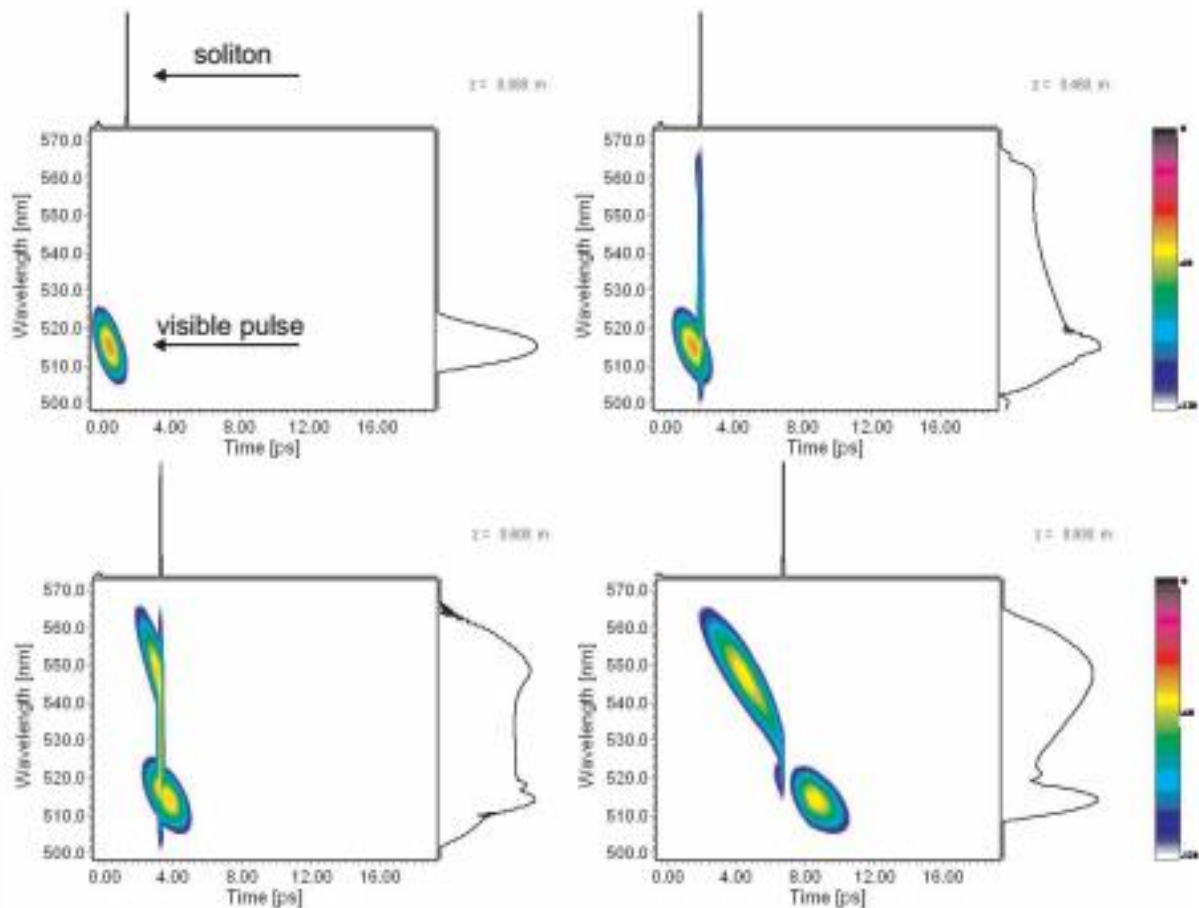
Figure 4: Simulation showing a soliton passing though the SH pulse. The leading edge of the soliton causes a redshift which is only partially compensated by the trailing edge because the red components walk away from the soliton. The simulation is made with a 150 fs, 0.1 nJ IR pulse and a 100 fJ, 300 fs green pulse and a relative delay of 5 ps. Time is relative to the pump at 1030 nm.

Numerical simulations based on the extended nonlinear Schrodinger equation confirm the energy conservation in the visible and clearly show how fundamental solitons pass through the visible pulse and cause XPM-shifts. The enhanced blue shift of the visible pulse with increasing IR pump power is a result of increased peak power of the first fundamental soliton At higher IR powers, the interaction becomes complicated as more solitons are formed and may overlap with the SH pulse. The physical origin of XPM is a change of the refractive index induced by a co-propagating optical pulse. XPM thus induces a frequency chirp given by

$$\partial\omega = -2\gamma \frac{\partial}{\partial T}|A,T|^2.dz$$

where $d\,z$ is the effective interaction length. Equation 1 shows that the trailing edge of an intense pulse will cause a blue shift of the co-propagating pulse whereas the leading edge will cause a redshift constant at 6 mW and the IR power is gradually increased up to 15 mW.
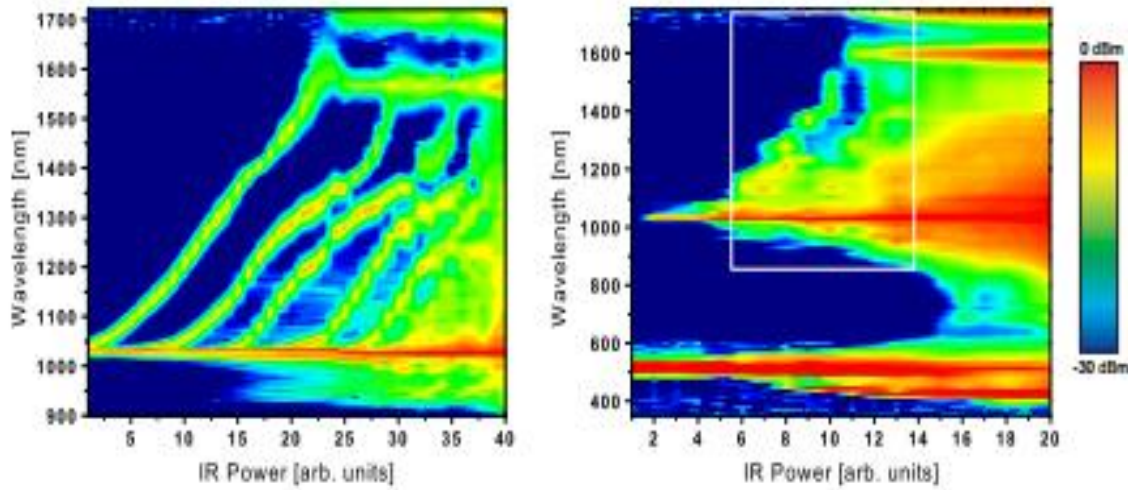
Figure .5: Left: Experimental spectral evolution with increasing power of the IR pulse. Right: Same evolution but with two pump wavelengths. The onset of significant blue-shifting of the SH pulse coincides with a red-shift of the first fundamental soliton to approximately 1200 nm. At this wavelength, the soliton has the same group velocity as the SH pulse

A soliton is a symmetric pulse so if a solution walks through another pulse its spectrum will be unchanged since each side of the soliton imposes equal but opposite phase shifts. However, if dispersion is present, the group velocity mismatch between the soliton and the XPM-shifted wavelength may cause them to separate temporally and thereby prevent the cancelling shift from the opposite side of the soliton. The result is a permanent XPM-shift - even if the soliton walk-through is complete. Figure 4 shows four frames from a simulation where a fundamental soliton passes through the visible pulse. In the second frame the leading edge of the soliton has caused a redshift of more than 50 nm. In the third and fourth frame, the trailing edge of the soliton blue shifts the previously red shifted components back again but, because of ispersion, some of the red intensity separates from the soliton and does not get shifted back.
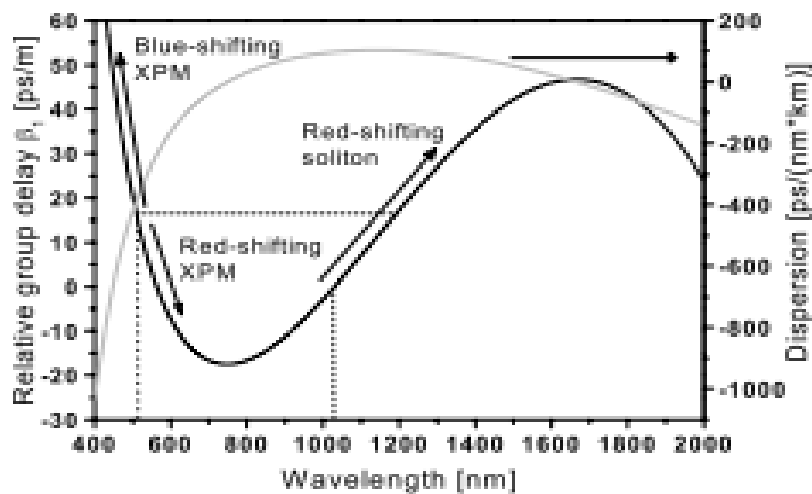

Figure 6: Calculated group delay relative to 1028 nm (black) and dispersion (gray). Red-shifting solitons slows down and are eventually caught by the SH pulse. With an appropriate temporal overlap between pulses, cascaded XPM can take place

The result is a permanent red- shift are shown for each IR power level and the figure clearly shows how isolated fundamental solitons are emitted and red-shifted as the input power is increased. Firstly, one soliton is formed and shifts towards the infrared. At higher power (spectrum ~ 10), a second soliton is emitted and so forth. Figure 5 (right) shows the same evolution but with the additional SH pulse launched into the fiber. The power of the green pulses is kept constant at a low power of 6 mW. No changes in the infrared spectra are observed due to the green pump pulse. In contrast, the spectrum of the 514 nm pulse is influenced significantly. After the first soliton is emitted, the spectrum of the green pulse starts to extend to the blue ("8" on power axis). At the highest IR power, the cascaded action of several solitons results in a maximum blue shift down to approximately 420 nm. Figure 6 shows the dispersion and the group delay relative to 1028 nm for the fiber under investigation. The relative group delay increases when the solitons redshift (they slow down), causing their group velocity to approach the group velocity of the SH pulse. This explains the size of the observed XPM-shifts - the enhanced temporal overlap increases the effective interaction length. The steep slope of the curve in the visible implies a large group velocity mismatch between the soliton and XPM-shifted components and the resulting walk-off is responsible for the permanent frequency shift. Since the results above apparently can be understood by simple analysis of the group delay curve, it is interesting to repeat the experiment with another fiber. Figure 7 shows the

dispersion and group delay relative to 1028 nm for the widely used NL-PM-750 (from Crystal Fibre). Comparison with figure 6 reveals an important difference between the group delays in the two fibers. In NL-PM-750 it is not possible for a red-shifting soliton to obtain the same group velocity as the SH pulse at 514 nm and the size of the XPM shift is therefore expected to be smaller than in the previous fiber. The soliton is always faster than the SH pulse so it is not possible to make the trailing edge of the solitons blue-shift the SH pulse. However, by delaying the soliton with respect to the SH pulse, it is possible for the faster soliton to catch up and walk through the visible pulse.
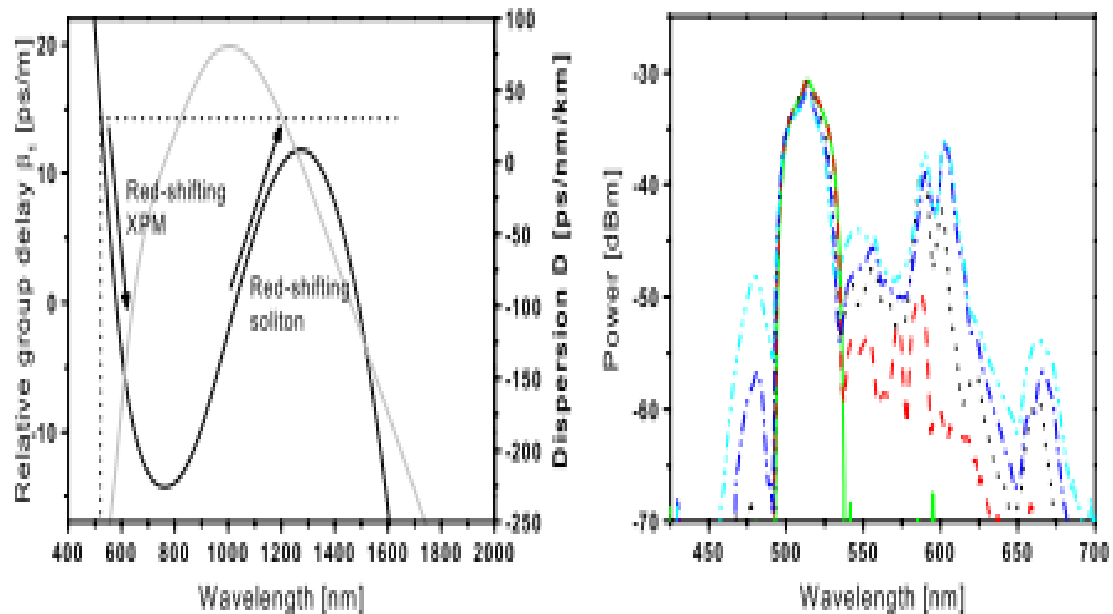

Figure 7: Left: Calculated group delays with respect to 1028 nm (black) and dispersion (gray). The red-shifting solitons are always faster than the SH pulse. Right: Measured spectral broadening in the visible as the IR power is increased. Regardless of the chosen delay it is not possible to induce a blue-shift. The blue peak at approximately 480 nm is NSR.
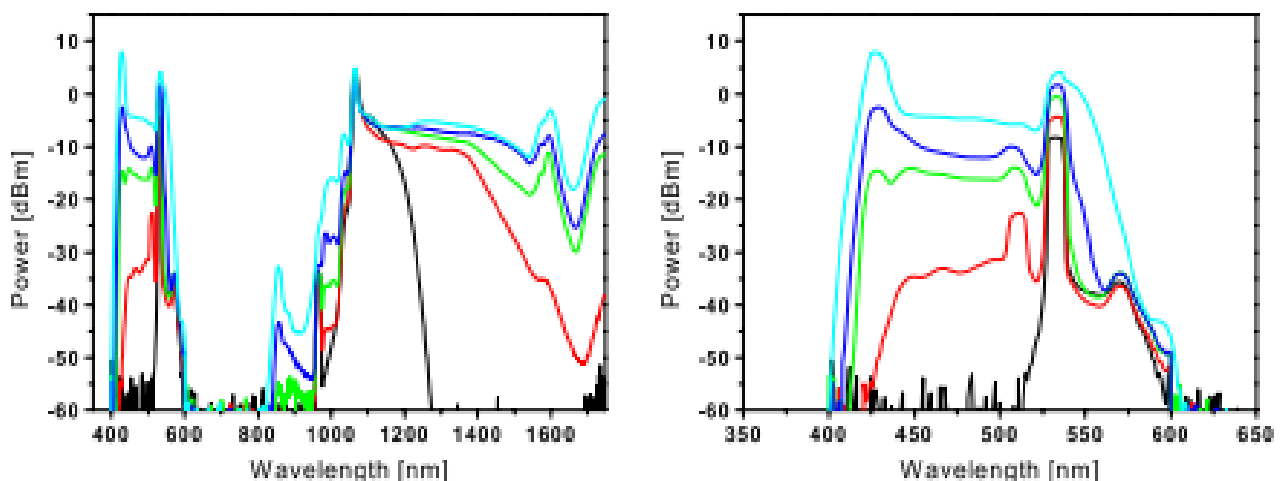

Figure 8: Left: Spectral evolution for increasing power. Right: Zoom on the visible part of the spectrum. Cascaded XPM leads to a significant blue-shift of the green pulse. The increased flatness in the visible is attributed to an increased number of solitons, each imposing XPM on the visible pulse. Data provided by Carsten Thomsen.

Group velocity mismatch then allows red-shifted components to escape from the soliton, leaving a permanent red-shift. Figure 7 (right) shows spectra obtained by femtosecond pumping of the fiber, which illustrates this point. Regardless of IR power and choice of delay, it is not possible to blue shift the visible pulse. The blue peak at 485 nm is emerging NSR, which grows as the soliton number increases. In conclusion, the outcome of the dual-wavelength pumping experiment can be understood by analyzing the group delay curve. The critical parameter is the group velocity mismatch between the XPM shifted components and the interacting soliton. For a given set of pump wavelengths, it is thus possible to calculate the obtainable frequency shift solely from the group velocity curve. Therefore new light sources can be developed by a proper choice of pump wavelengths and suitable design of the fiber dispersion.

PICOSECOND DUAL-WAVELENGTH PUMPING

Similar experiments with picosecond pulses have been made by Carsten Thomsen from NKT-Research. A fiber oscillator, delivering 5 picosecond pulses at 1060 nm at a repetition rate of 80 MHz, was used to drive a setup like the one presented in figure 1. The results are remarkably similar to the ones obtained by femtosecond pumping as seen by comparison of figure 8 and figure 3 (same fiber). Again, integration of spectra and numerical simulations show that there is no energy transfer from the IR to the visible. The blue-shifted components in figure 8 originate from the SH pulse and are merely spectrally shifted by the IR pulse. It has previously been shown that picosecond pulses, as well as nanosecond pulses, break up into very short pulses due to modulation instabilities in presence of negative GVD.
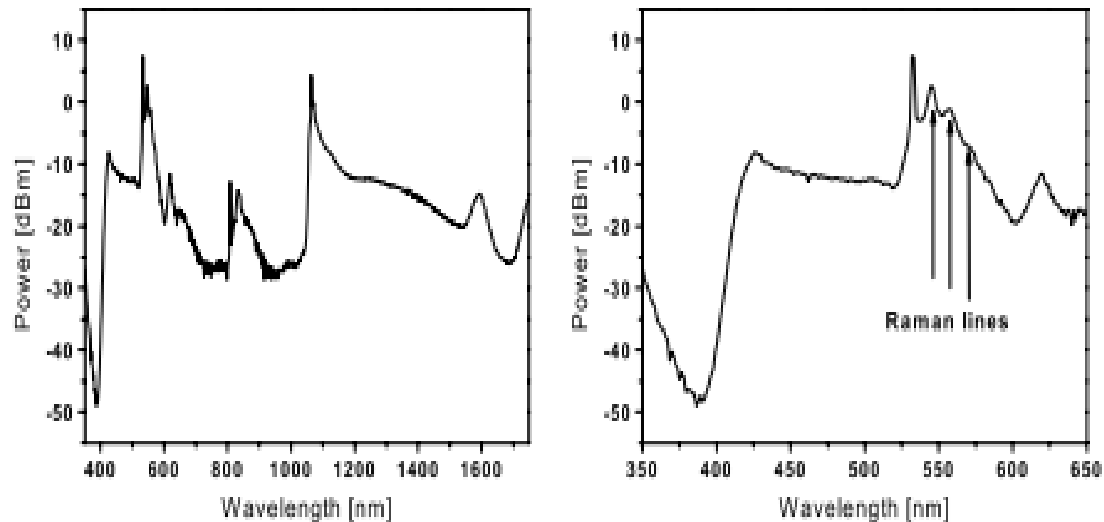

Figure 9: Left: Spectrum from nanosecond dual-wavelength pumping. The sharp feature at 808 nm is residual pump from the microchip cavity. Right: A flat plateau extends from 420 nm to 540 nm. The bumps to the right of the 530 nm pump are 13.2 THz shifted Raman-peaks. Curves provided by Yujun Qian, NKT-Research

The short pulses subsequently form solitons, which then evolve as described in the previous section. So, although other nonlinear effects such as FWM and SRS may contribute to the spectral broadening   the governing mechanism is still soliton fission and soliton XPM. In comparison to the femto second scenario the only important difference is the number of solitons created. As the soliton number scales with the pulse duration, a picosecond pulse will split into a much higher number of solitons. This implies a complicated interaction with the SH pulse as there will be many XPM-shifts from several solitons. This explains the improved flatness of the spectra in figure 8 compared to the spectra shown in figure 3. It should be noted that the spectra in figure 8 also contains a contribution at 420 nm from NSR. The presence of NSR shows that soliton fission is indeed taking place.

NANOSECOND DUAL-WAVELENGTH PUMPING

 Considering the results presented above, it is not surprising that nanosecond pumping of the fiber leads to similar results as for femtosecond and picosecond pumping. A nanosecond pulse launched in the anomalous regime will break up into short pulses due to modulation instabilities and (many) solitons will be created. As before, the XPM interaction of the SH and the fundamental solitons cause a frequency shift of the SH pulse and create a continuum with high spectral density in the blue part of the spectrum. The resulting spectra of such an experiment are shown in figure 9. The similarity with the previous results indicates that soliton dynamics play a key role, and the flat spectrum and merging of discrete Raman lines can be explained by the XPM induced shifts imposed by numerous solitons. Again, the presence of NSR indicates that soliton fission is taking place, which further validates this suggestion. The use of nanosecond pump pulses is highly attractive from a practical point of view as it enables use of compact microchip pump sources. Passive Q switching of such lasers has been shown to enable few-nanosecond pulses with peak powers in the kW range. Dual-pump setups can thus be made in extremely compact form employing relatively simple components and such a setup is the basis of the Super K-Blue white-light source. The drawback of nanosecond pumping is the relatively high pulse energies which can cause damage to the fiber. As a consequence, the average power is limited to about 50 mW. High repetition rate picosecond or femtosecond pumping would remove this constraint and allow higher average power. The price is show ever added complexity of the setups.

REFERENCES

1. P. P´erez-Mill´an, A. Diez, M. V. Andr´es, D. Zalvidea, and R. Duchowicz, "Q-switched all-fiber laser based on magnetostriction modulation of a Bragg Grating," Opt. Express (2005).
2. R. Kashyap, *Fiber Bragg Gratings* (Academic Press, 1999).
3. Y. Wang and C. Q. Xu, "Switching-induced perturbation and influence on actively Q-switched fiber lasers," J. Quantum Electronics 40, 1583–1596 (2004).
4. G. Agrawal, *Applications of nonlinear fiber optics* (Academic Press, 2001).
5. C. C. Cutler, "Why does linear phase shift cause mode-locking?" J. Quantum Electronics.
6. D. Huang, W. Liu, and C. C. Yang, "Q-switched all-fiber laser with an acoustically modulated fiber attenuator," IEEE Phot. Tech. Lett.1153–1155 (2000).
7. Y. Sintov, O. Katz, Y. Glick, S. Acco, Y. Nafcha, A. Englander, and R. Lavi, "Extractable energy from Ytterbium-doped high-energy pulsed fiber amplifiers and lasers," J. Opt. Soc. Am. B 23, 218 (2006).
8. H. Deyerl, N. Plougmann, J. B. Jensen, F. Floreani, H. R. Sørensen, and M. Kristensen, "Fabrication of advanced Bragg gratings with complex apodization profiles by use of the polarization control method," J. Appl. Optics 43, 3513 (2004).
9. D. Ouzounov, D. Homoelle, W. Zipfel, W. W. Webb, A. L. Gaeta, J. A. West, J. C. Fajardo, and K. W. Koch, "Dispersion measurements of microstructured fibers using femtosecond laser pulses," Opt. Com.
10. D. M¨uller, J. West, and K. Koch, "Interferonmetric chromatic dispersion measurement of a photonic band-gap fiber," Proceedings of Spie, Active and Passive Optical Components for WDM Communications II 4870 (2002).
11. A. Isom¨aki and O. G. Okhotnikov, "All-fiber Ytterbium soliton modelocked laser with dispersion control by solid-core photonic bandgap fiber," Opt. Express 14, 4368 (2006).
12. P. Champert, V. Couderc, P. Leproux, S. F´evrier, V. Tombelaine, L. Labont´e, P. Roy, C. Froehly, and P. N´erin, "White-light supercontinuum generation in normally dispersive optical fiber using original multiwavelength pumping system," Opt. Express 12, 4366–4371 (2004).
13. G. P. Agrawal, P. L. Baldeck, and R. R. Alfano, "Temporal and spectral effects of cross-phase modulation on copropagating ultrashort pulses in optical fibers," Phys. Rev. 5063–5072 (1989).
14. A. V. Husakou and J. Herrmann, "Supercontinuum generation, four-wave mixing, and fission of higher-order solitons in photonic crystal fibers," J. Opt. Soc. Am.
15. T. Schreiber, J. Limpert, H. Zellmer, A. T¨unnermann, and K. P. Hansen, "High average power supercontinuum generation in photonic crystal fibers," Opt. Commun. 71–78 (2003).
16. G. Cerullo and S. Silvestri, "Ultrafast optical parametric amplifiers," Review of Scientific Instruments.
17. G. M. Gale, M. Cavallari, T. J. Driscoll, and F. Hache, "Sub-20 fs pulses tunable pulses in the visible from an 82 MHz optical parametric oscillator," Opt. Lett 1562–1564 (1995).
18. R. Danielius, A. Piskarskas, A. Stabinis, G. P. Banfi, P. D. Trapani, and R. Righini, "Travelling-wave parametric generation of widely tunable highly coherent femtosecond light pulses," J. Opt. Soc. Am. B.
19. S. Barkus, C. G. Durfee, M. M. Murnane, and H. C. Kapteyn, "High power ultrafast lasers," Review of Scientific Instruments 69, 1207–1223 (1998)
20. L. Goldberg, J. P. Koplow, and D. A. V. Kliner, "Highly efficient 4-W Ybdoped fiber amplifier pumped by a broad-stripe laser diode," Opt. Lett. 673–675 (1999).
21. J. A. Armstrong, N. Bloembergen, J. Ducuing, and P. S. Pershan, "Interaction between light waves in nonlinear dielectric," Phys. Rev. 1918–1939 (1962).